

RESEARCH ARTICLE

# Involvement of Intracellular and Mitochondrial A $\beta$ in the Ameliorative Effects of Huperzine A against Oligomeric A $\beta$ <sub>42</sub>-Induced Injury in Primary Rat Neurons

Yun Lei<sup>1</sup>, Ling Yang<sup>1</sup>, Chun Yan Ye<sup>1</sup>, Ming Yan Qin<sup>2</sup>, Huai Yu Yang<sup>2</sup>, Hua Liang Jiang<sup>2</sup>, Xi Can Tang<sup>2</sup>, Hai Yan Zhang<sup>2\*</sup>

**1** CAS Key Laboratory of Receptor Research, Shanghai Institute of Materia Medica, Chinese Academy of Science, Shanghai, China, **2** Drug Discovery and Design Center, State Key Laboratory of Drug Research, Shanghai Institute of Materia Medica, Chinese Academy of Sciences, Shanghai, China

\* [hzhang@simmm.ac.cn](mailto:hzhang@simmm.ac.cn)



**OPEN ACCESS**

**Citation:** Lei Y, Yang L, Ye CY, Qin MY, Yang HY, Jiang HL, et al. (2015) Involvement of Intracellular and Mitochondrial A $\beta$  in the Ameliorative Effects of Huperzine A against Oligomeric A $\beta$ <sub>42</sub>-Induced Injury in Primary Rat Neurons. PLoS ONE 10(5): e0128366. doi:10.1371/journal.pone.0128366

**Academic Editor:** Donghui Zhu, North Carolina A&T State University, UNITED STATES

**Received:** January 15, 2015

**Accepted:** April 26, 2015

**Published:** May 29, 2015

**Copyright:** © 2015 Lei et al. This is an open access article distributed under the terms of the [Creative Commons Attribution License](https://creativecommons.org/licenses/by/4.0/), which permits unrestricted use, distribution, and reproduction in any medium, provided the original author and source are credited.

**Data Availability Statement:** All relevant data are within the paper and its Supporting Information files.

**Funding:** This work was supported by the National Natural Science Foundation of China (No 81173034), the National Science & Technology Major Project "Key New Drug Creation and Manufacturing Program" of China (No. 2012ZX09301001-004), and the Ministry of Science and Technology of China (No 2011CB510004).

**Competing Interests:** The authors have declared that no competing interests exist.

## Abstract

Considerable studies indicate huperzine A is a promising natural product to suppress neuronal damages induced by  $\beta$ -amyloid (A $\beta$ ), a key pathogenic event in the Alzheimer's disease (AD). As an extension, the present study for the first time explored whether the beneficial profiles of huperzine A against oligomeric A $\beta$ <sub>42</sub> induced neurotoxicity are associated with the accumulation and detrimental function of intraneuronal/mitochondrial A $\beta$ , on the basis of the emerging evidence that intracellular A $\beta$  is more relevant to AD progression as compared with extracellular A $\beta$ . Huperzine A treatment was shown to significantly attenuate the neurotoxicity of oligomeric A $\beta$ <sub>42</sub>, as demonstrated by increased neuronal viability. Interestingly, our results proved that exogenous A $\beta$ <sub>42</sub> could accumulate intraneuronally in a dose- and time-dependent manner, while huperzine A treatment markedly reduced the level of intracellular A $\beta$ <sub>42</sub>. Moreover, huperzine A treatment rescued mitochondrial dysfunction induced by oligomeric A $\beta$ <sub>42</sub>, including adenosine triphosphate (ATP) reduction, reactive oxygen species (ROS) overproduction and membrane potential depolarization. Further study demonstrated that huperzine A also significantly reduced the level of A $\beta$ <sub>42</sub> in the mitochondria-enriched subcellular fractions, as well as the A $\beta$ <sub>42</sub> fluorescent signals colocalized with mitochondrial marker. This study indicates that interfering intracellular A $\beta$  especially mitochondrial A $\beta$  accumulation, together with ameliorating A $\beta$ -associated mitochondrial dysfunction, may contribute to the protective effects of huperzine A against A $\beta$  neurotoxicity. Above results may shed more light on the pharmacological mechanisms of huperzine A and provide important clues for discovering novel therapeutic strategies for AD.

## Introduction

AD, the most common cause of dementia, is a chronic disorder characterized by progressive decline in cognitive function [1]. Compelling evidence shows that excessive accumulation of A $\beta$  peptide in the brain is a central and perhaps defining event in the pathogenesis of AD [2, 3], thus “A $\beta$  cascade hypothesis” is strongly supported by evidence of A $\beta$ -related pathology and has been the focal point of research and pharmaceutical industry for the past twenty years [2, 4]. Although the precise molecular mechanisms behind A $\beta$ -associated neurotoxicity remain to be elucidated, increasing evidence indicates that intracellular accumulation of A $\beta$  is more relevant to AD process as compared with extracellular A $\beta$  [5, 6]. Intracellular A $\beta$  has been proposed as an early event in AD pathogenesis, which is built up by intracellular A $\beta$  generation and reuptake of secreted A $\beta$  from extracellular environment [7]. Recent researches show that intracellular A $\beta$  plays a pivotal role in AD-associated malignant changes, including tau phosphorylation [8], reduction in synaptic protein expression [9], and mitochondrial dysfunction [10]. Afore-mentioned evidence has raised the prospect of discovering effective therapeutic strategies on blocking A $\beta$  internalization from the extracellular space or its intracellular accumulation, especially under the circumstance that current pharmacological approaches against A $\beta$  formation or immunization failed to gain promising efficacy on preventing and/or delaying AD progressing.

Huperzine A, a *Lycopodium* alkaloid isolated from Chinese folk medicine *huperzia serrata* (Qian Ceng Ta), has been proven to effectively attenuate cognitive deficits and is widely used for AD treatment in China [11, 12]. Recent studies indicate that huperzine A can effectively alleviate A $\beta$ -associated neurotoxicity in many *in vitro* and *in vivo* models, besides its potent acetylcholinesterase (AChE) inhibitory effect [12, 13]. Huperzine A has been proven to rescue A $\beta_{25-35}$  induced oxidative stress and apoptosis in rat pheochromocytoma cells [14], NG108-15 cells [15], and rat cortical neurons [16]. Nevertheless, the precise molecular mechanisms underlying the protective effects of huperzine A against A $\beta$ -associated neuronal dysfunction have not been well clarified yet. As strong evidence accumulated in recent years indicates that A $\beta$  oligomers, rather than A $\beta$  fibrils or monomers, are the prominent neurotoxins in AD pathology [17–19], the current work for the first time employed oligomeric A $\beta_{42}$  to determine the ameliorative effect of huperzine A against A $\beta$ -induced injury in primary cortical neurons and explore whether this effect is associated with intracellular A $\beta$ .

Recently, a number of studies have brought up the close association between intracellular A $\beta$  and mitochondrial dysfunction [20]. Intracellular A $\beta$  can be taken up by mitochondria through the TOM machinery and MAM connection [21], and hence mitochondria become one of the major subcellular pools of A $\beta$  [22]. Moreover, many studies have provided substantial evidence for the direct links between progressive accumulation of mitochondrial A $\beta$  and mitochondrial dysfunction [20, 23], including abnormal ATP production, oxidative stress and membrane potential damage [24]. Taken together the potential effects of huperzine A on mitochondrial dysfunction in various models [14, 16], it will be therefore of great interest to clarify whether the mitochondrial function and mitochondrial A $\beta$  level are also influenced by huperzine A treatment in oligomeric A $\beta_{42}$ -associated primary cortical neuronal model.

## Materials and Methods

### Ethics Statement

The animal works and experiment protocols were approved by the Institutional Animal Care and Use Committee of Shanghai Institute of Materia Medica. All the Sprague Dawley (SD) rats were obtained from Shanghai Laboratory Animal Center, Chinese Academy of Science, and

maintained in the specific pathogen-free and Association for Assessment and Accreditation of Laboratory Animal Care International (AAALAC) approved animal facility under 20–26°C temperature and 40–70% humidity with 12 h light/dark cycles.

## Materials

Huperzine A (purity > 99%, Wan Bang Pharmaceutical Co.Ltd.) was dissolved in 0.1 N HCl at 5 mg/ml as stock solution, and diluted to proper concentrations before usage with neurobasal medium. Stock solution of A $\beta$ <sub>42</sub> (Millipore) was prepared in 100% DMSO at a concentration of 5 mM, and then diluted to 10  $\mu$ M with neurobasal medium and aged for 24 hours at 4°C to prepare oligomeric A $\beta$ <sub>42</sub>. The aggregation state of prepared oligomeric A $\beta$ <sub>42</sub> was characterized by atomic force microscope (AFM) and western blotting (Figure A in [S1 File](#)), which showed the similar oligomeric forms as the observation of other labs [25, 26]. All stock solutions were stored at -20°C. All the other chemicals and reagents were purchased from Sinopharm Chemical Reagent Co.Ltd., unless otherwise stated.

## Primary cortical neuron culture and drug treatment

Cortical neurons were isolated from E16-E17 SD rat embryos according to the method described by Lu's lab [27] with slight modification. Briefly, cortices were dissected in cold high glucose Dulbecco's Modified Eagle's Medium (HG-DMEM, Invitrogen), dissociated with 0.125% (w/v) trypsin at 37°C for 15 minutes, and then triturated with pipette in HG-DMEM with 10% (v/v) fetal bovine serum (FBS, Gibco). After non-dispersed tissue settled for 2 minutes, the supernatants were filtered through strainer (300/400 mesh) and transferred to a new tube. Then, the cell suspension was diluted into optimal concentration ( $6 \times 10^5$  cells/well for 6-wells plate,  $3 \times 10^4$  cells/well for 96-wells plate,  $1.5 \times 10^5$  cells/slide) with HG-DMEM containing 10% FBS and plated onto poly-L-lysine (Sangon Biotech)-coated plates or slides. Four hours later, the culture medium was completely removed, and the cells were cultured in neurobasal medium (Invitrogen) with 0.5 mM L-glutamine, 2% (v/v) B27 supplement, penicillin (60 mg/L) and streptomycin (50 mg/L). No mitosis inhibitors were used. Half of the culture medium was refreshed every 3 days. Following 9 days of culture, the purity of primary cultured neurons was assessed by immunocytochemical technique using Tau as neuronal marker and GFAP as glial marker [28], which revealed that the majority of cultured cells were neurons (data not shown). Neurons were pretreated with 1  $\mu$ M oligomeric A $\beta$ <sub>42</sub> or HiLyte Fluor 488-labeled-A $\beta$ <sub>42</sub> (HiLyte-A $\beta$ <sub>42</sub>, AnaSpec) for 2 hours and then incubated with 0, 0.1, 1 or 10  $\mu$ M huperzine A for another 22 hours, while the vehicle-treated control group was treated with same amount of neurobasal medium.

## MTT assay

After treatment, 3-(4,5-Dimethylthiazol-2-yl)-2,5-diphenyltetrazolium bromide (MTT, Amresco) was added to culture medium at final concentration of 0.5 mg/ml and incubated at 37°C for 3 hours. The medium was removed after incubation, 100  $\mu$ L/well DMSO was then added to dissolve the formazan. Cell plates were shaken for 5 minutes and the absorbance of each well was measured with a PerkinElmer microplate reader at 490 nm. The absorbance value was normalized against the value of vehicle-treated control group.

## SRB assay

Sulforhodamine B (SRB) assay relies on the ability of SRB binding to protein components. After treatment, cells were fixed with 10% trichloroacetic acid for 1 hour at 4°C. Then, plates

were washed with H<sub>2</sub>O and air-dried. Cells were stained with 0.4% SRB in 1% acetic acid for 30 minutes at room temperature. Plates were washed with 1% acetic acid and air-dried. The stained cells were lysed in 10 mM Tris buffer and the absorbance was measured at 550 nm with a PerkinElmer microplate reader. The absorbance value was normalized against the value of vehicle-treated control group.

### Detection of neuronal ATP production

The ATP level of neurons was measured using a bioluminescent ATP detection kit (Promega). Briefly, cells were placed at room temperature for 30 minutes, and then lysed by adding 100  $\mu$ l of ATP-releasing reagent. The lysates were incubated with the luciferin substrate and luciferase enzyme in the dark for 10 minutes to stabilize the luminescent signal. The intensity of bioluminescence was measured using a PerkinElmer microplate reader. The bioluminescence intensity was normalized by control group and presented as the relative ATP level [23].

### Measurement of ROS level

ROS were measured based on the oxidation of 2', 7'-dichlorodihydrofluorescein diacetate (H<sub>2</sub>DCF-diacetate, Molecular Probes) to fluorescent DCF [29]. After treatment, cells were incubated in darkness with 10  $\mu$ M H<sub>2</sub>DCF-diacetate for 45 minutes at 37°C in NaCl-medium (132.0 mM NaCl, 4.0 mM KCl, 1.0 mM CaCl<sub>2</sub>, 1.4 mM MgCl<sub>2</sub>, 1.2 mM NaH<sub>2</sub>PO<sub>4</sub>, 6.0 mM glucose, 10.0 mM HEPES, pH 7.4). After two washes with above medium, cultured cells were solubilized with 1% SDS buffer (1% SDS, 5 mM Tris-HCl, pH 7.4). The intensity of DCF fluorescence in the lysate was measured using a PerkinElmer microplate reader with 485 nm excitation and 520 nm emission filters. The fluorescence intensity was normalized by control group and presented as the relative ROS level [30].

### Fluorimetric analysis of mitochondrial membrane potential

Mitochondrial membrane potential was measured using the fluorescent cationic dye JC-1 (Molecular Probes). After treatment, cells were incubated with the JC-1 (0.1  $\mu$ g/ml) at 37°C for 15 minutes and washed with PBS. The fluorescence intensity of JC-1 aggregates was detected with 520 nm excitation and 590 nm emission filters (red fluorescence), whereas the fluorescence intensity of the JC-1 monomers was measured with 485 nm excitation and 520 nm emission filters (green fluorescence) using a PerkinElmer microplate reader. The fluorescence intensity ratio of aggregates to monomers (red fluorescence to green fluorescence) was calculated as an indicator of mitochondrial membrane potential ( $\Delta\Psi_m$ ). The  $\Delta\Psi_m$  was presented as the percentage of control group [31].

### Protein extraction and western blotting

For total cellular protein extraction, cells were washed twice with ice-cold PBS and lysed in RIPA buffer (50 mM Tris-HCl, 150 mM NaCl, 0.5% sodium deoxycholate, 1% Triton X-100, 0.1% sodium dodecyl sulfate, 1 mM NaF, 1 mM Na<sub>3</sub>VO<sub>4</sub>, 1 mM PMSF, 1% P8340, pH 7.4), followed by centrifugation at 12,000 g for 15 minutes at 4°C. Protein concentration of supernatants was measured using a BCA assay kit (Pierce).

The protein samples were mixed with Loading buffer without DTT and separated in 4%/10%/17% gradient Tricine-SDS-PAGE gels for A $\beta$  blotting. The proteins were subsequently transferred to the nitrocellulose membrane. Blots were blocked with 5% nonfat milk for 1 hour at room temperature before incubation overnight with primary antibodies: A $\beta$  (6E10, Covance, SIG-39320, mouse monoclonal antibody, 1:1000 dilution),  $\beta$ -actin (Sigma Aldrich, A5441,

mouse monoclonal antibody, 1:10000 dilution). Blots were washed with Tris-buffered saline buffer containing 0.05% Tween-20, incubated with a horseradish peroxidase-conjugated anti-mouse antibody (Kangcheng, 1:5000) for 1 hour at room temperature, and then detected using the ECL plus detection kit (Amersham GE Healthcare). The immunoreactive bands were visualized by autoradiography, and the intensity of each band was quantified with Image J software.

### Intracellular and mitochondrial A $\beta_{42}$ level measurement

Intracellular A $\beta_{42}$  level was determined by ELISA kit (Invitrogen) according to the manufacturer's instruction. The whole cell lysates were diluted 300 times (v/v) with ELISA dilution buffer and used as samples for ELISA. According to our experimental result, the residual amount of RIPA buffer in ELISA samples did not influence the ELISA assay (data not shown).

The mitochondria-enriched fractions were prepared according to the method described by Yan's lab [32] with slight modification. Briefly, after treatment, cells were washed twice with ice-cold PBS and harvested in ice-cold PBS using flat-cell scrapers, and centrifuged for 5 minutes at 300 g (4°C) to collect cells. The cell deposits were gently homogenized 10 times using a Dounce homogenizer in 200  $\mu$ L sucrose-based lysis buffer (50 mM Tris, 1 mM EDTA, 1 mM EGTA, 250 mM sucrose, 1 mM PMSF, 1% P8340, pH 7.4). The lysates were centrifuged at 750 g for 10 minutes (4°C) to remove nuclei and cell debris. The supernatants were centrifuged at 10,000 g for another 15 minutes (4°C). RIPA buffer (30  $\mu$ L) was added to suspend the resulting pellets and the lysate was used as mitochondria-enriched fraction. Centrifuged the resulting supernatants at 105,000 g for 60 minutes (4°C). The final supernatants were used as cytosolic fraction. The final pellets were re-suspended with 50  $\mu$ L RIPA buffer and used as membrane-enriched fraction. The purity of subcellular fractions was detected using western blotting (Figure B in [S1 File](#)). After appropriate dilution, the samples and standards were measured according the manual of ELISA kit. Absorbance at 450 nm was measured using a PerkinElmer microplate reader. The protein content of each sample was detected using a BCA assay kit. A $\beta_{42}$  level was calculated from the standard curve and presented as ng/mg protein or the percentage of A $\beta_{42}$ -treated group.

### Confocal microscopy observation of intracellular A $\beta$ distribution

After treatment with HiLyte-A $\beta_{42}$ , the media were removed and cells were incubated with pre-warmed (37°C) solution containing mitotracker probe (250 nM, Invitrogen) for 45 minutes under growth condition. After washing twice with PBS, the cells were fixed with PBS containing 4% paraformaldehyde. The fixed cells were further incubated with 4', 6-diamidino-2-phenylindole (DAPI, 1  $\mu$ g/ml) to label nuclei and rinsed three times with PBS. The confocal images were obtained with Olympus FV1000-IX81 microscope, using the vendor-provided software (OLYMPUS FLUOVIEW Ver.2.1b Viewer). Fluorescence intensity was quantified with Image J software and presented as the percentage of HiLyte-A $\beta_{42}$ -treated group.

### Statistical analysis

All data were presented as mean  $\pm$  SEM. Results of MTT assay and SRB assay were analyzed using one-way ANOVA with the Dunnett's test, and the other results were analyzed using Student's t-test. For all statistical tests,  $p < 0.05$  was considered significant.

## Results

### Huperzine A alleviated oligomeric A $\beta_{42}$ induced damage in the primary rat neurons

In order to evaluate the effect of huperzine A on oligomeric A $\beta_{42}$  induced neurotoxicity, here we employed MTT assay and SRB assay on primary cortical neurons. The MTT absorbance of neurons decreased to 60% of control group upon incubation with 1  $\mu$ M oligomeric A $\beta_{42}$  (Fig 1A,

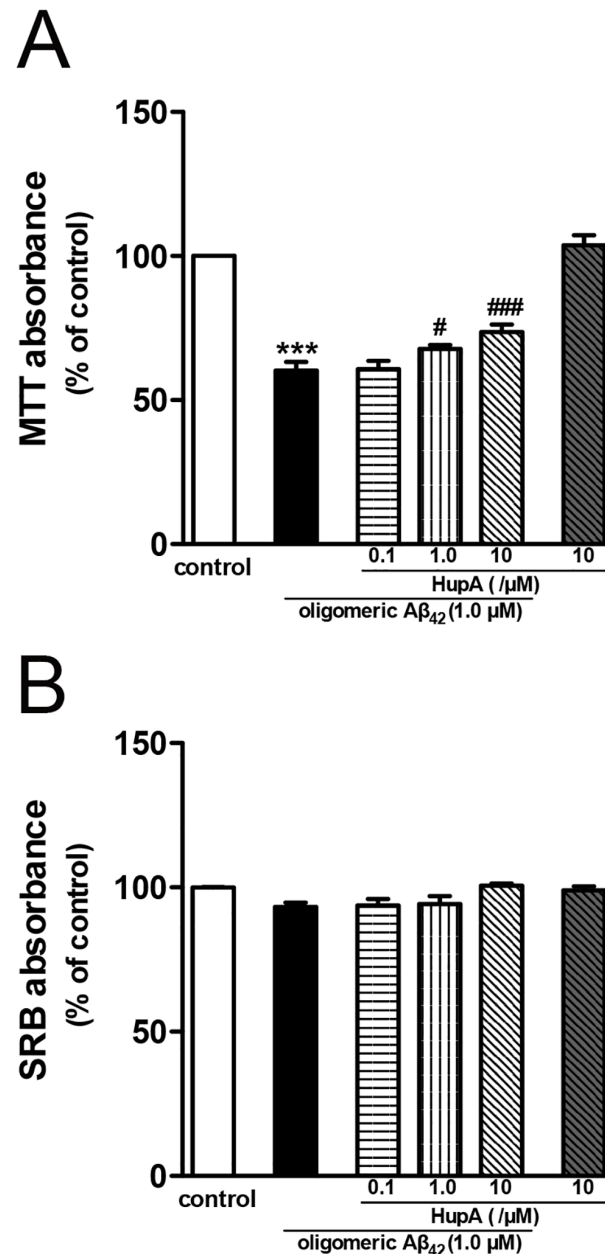


**Fig 1. Huperzine A ameliorated oligomeric A $\beta_{42}$  induced damage in primary rat neurons.** **A.** The results of MTT assay (N = 6). **B.** The results of SRB assay (N = 3). Data were presented as percentage of control group, and shown as mean  $\pm$  SEM. \*\*\*p < 0.001 vs control group; #p < 0.05, ###p < 0.001 vs oligomeric A $\beta_{42}$ -treated group. Huperzine A was abbreviated as HupA.

doi:10.1371/journal.pone.0128366.g001

$p < 0.001$  vs vehicle-treated control group), while post-treatment with 1  $\mu\text{M}$  or 10  $\mu\text{M}$  huperzine A markedly increased the MTT absorbance (Fig 1A,  $p < 0.05$  and  $p < 0.001$  vs A $\beta_{42}$ -treated group, respectively). No significant difference was observed between control group and huperzine A without oligomeric A $\beta_{42}$ -treated group ( $p > 0.05$ ). As shown in Fig 1B, there was no significant difference of the SRB absorbance between oligomeric A $\beta_{42}$ -treated group and vehicle-treated control group ( $p > 0.05$ ). Huperzine A treatment did not change the SRB absorbance either ( $p > 0.05$ ). We chose 10  $\mu\text{M}$  huperzine A to carry out the subsequent experiments.

### Huperzine A decreased intracellular A $\beta_{42}$ accumulation

Intracellular A $\beta$  plays an important role in A $\beta$  induced neuronal toxicity [7]. To evaluate whether huperzine A could influence the level of intracellularly accumulated A $\beta$ , we measured the level of A $\beta$  in cell lysate by ELISA using an antibody specific for the NH<sub>2</sub>-terminus region of human A $\beta$  (Invitrogen) to distinguish it from endogenous rat A $\beta$ . As shown in Figure C in S1 File, A $\beta_{42}$  accumulated in neurons in a dose- and time-dependent manner, whereas the A $\beta_{42}$  of vehicle-treated neurons was at background level. The level of intracellular A $\beta_{42}$  correlated well with the cell viability (Figure C in S1 File,  $R^2 = 0.98$ ,  $p < 0.001$ ). Huperzine A treatment significantly decreased the level of intracellular A $\beta_{42}$  (Fig 2A,  $p < 0.05$  vs oligomeric A $\beta_{42}$ -treated group). We also employed western blotting to evaluate the level and form of A $\beta$  in cell lysate. As shown in Fig 2B and 2C, huperzine A-treated neurons displayed lower A $\beta_{42}$  immuno-intensity as compared with vehicle-treated neurons ( $p < 0.05$  vs oligomeric A $\beta_{42}$ -treated group), which was comparable to the results of ELISA. Similar decreasing tendencies were found in the changes of A $\beta$  dimer, trimer and tetramer level ( $p < 0.01$  for dimer and trimer,  $p < 0.05$  for tetramer, Fig 2C), which are the normally recognized toxic forms of synthetic A $\beta$  oligomers [17, 33–35]. Interestingly, there was an obvious band (between 37 kD and 50 kD) existed in the immunoblots of both A $\beta$  exposed alone group and A $\beta$ -exposed with huperzine A post-treatment group, which was marked with asterisk (Fig 2B). Considering this band also existed in the non-A $\beta$ -treated cell lysate (Figure D in S1 File), it is mostly likely to be a nonspecific signal of 6E10 antibody. To be in agreement, similar phenomenon was also observed in other literature [36]. Nevertheless, the existing of this nonspecific band did not affect the experimental outcome as the intensity of total detected bands, including or excluding the nonspecific bands, showed comparable decrease in huperzine A-treated group (Fig 2C). Above results obtained through ELISA and western blotting suggested that huperzine A decreased intracellular A $\beta$  accumulation.

To make further confirmation, we applied HiLyte-A $\beta_{42}$  [37, 38] on neurons. HiLyte-A $\beta_{42}$  was proved to possess similar neuronal toxicity as compared with previous A $\beta_{42}$  in MTT assay (Data not shown). As shown in Fig 2D and 2E, huperzine A treatment decreased the intracellular HiLyte-A $\beta_{42}$  fluorescence intensity ( $p < 0.05$  vs oligomeric A $\beta_{42}$  treated group), which was similar as the results obtained by ELISA and western blotting.

### Huperzine A ameliorated oligomeric A $\beta_{42}$ induced mitochondrial dysfunctions in primary cortical neurons

Mitochondrial dysfunction is largely involved in the intracellular A $\beta$  toxicity [22]. We therefore conducted a series of assays to evaluate the mitochondrial function of oligomeric A $\beta_{42}$ -exposed neurons treated with or without huperzine A. The cellular ATP level was firstly measured to evaluate the mitochondrial function. As an energy storage and transfer molecule, ATP was mostly synthesized in the mitochondria. Using a luciferin-luciferase assay, we observed that the ATP level of oligomeric A $\beta_{42}$  treated group reduced obviously as compared with the control group (Fig 3A,  $p < 0.01$  vs vehicle-treated control group). Huperzine A significantly

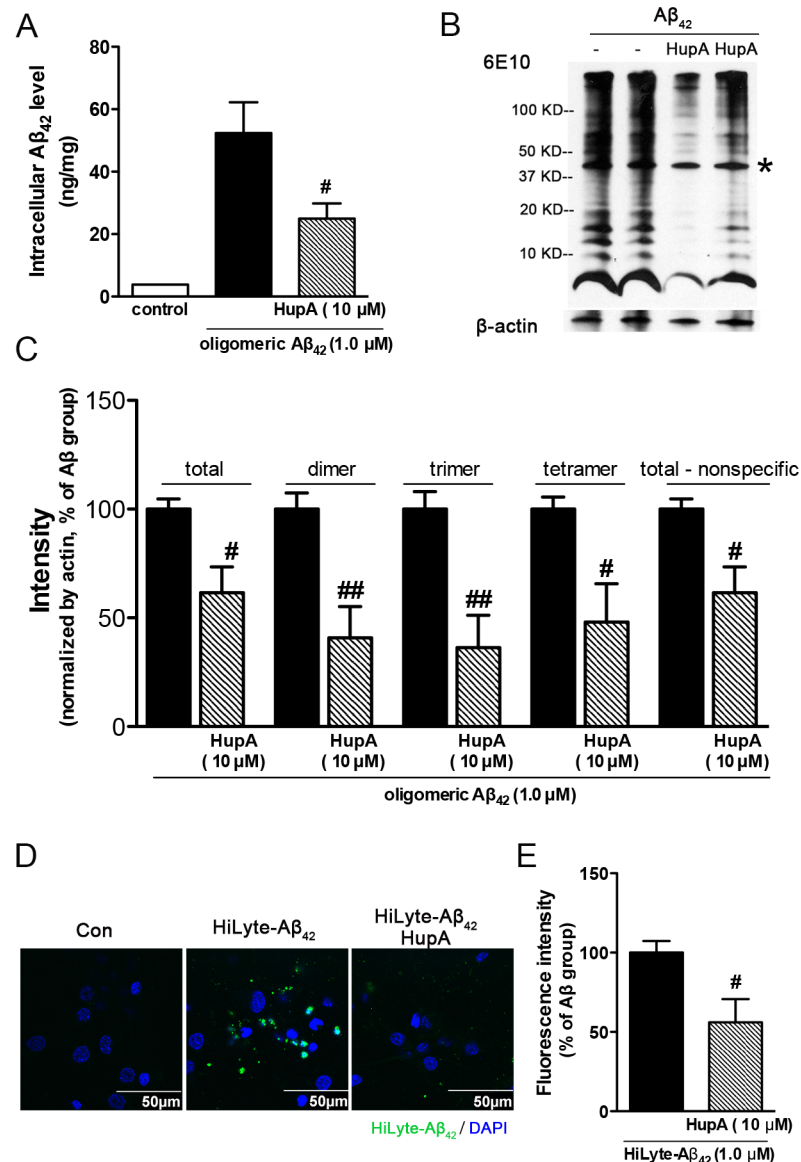


**Fig 2. Huperzine A decreased intracellular A $\beta_{42}$  accumulation.** Intracellular A $\beta_{42}$  level and/or form were measured by ELISA (A, N = 4) and western blotting (B). C. The statistical result of western blotting (N = 3). D. The representative figures of primary neurons exposed to HiLyte-A $\beta_{42}$ . E. The statistical result of HiLyte-A $\beta_{42}$  fluorescence intensity (N = 4). Data were shown as mean  $\pm$  SEM. Asterisk denoted the non-specific band detected by the 6E10 antibody. <sup>#</sup>p < 0.05 vs oligomeric A $\beta_{42}$ -treated group or HiLyte-A $\beta_{42}$  treated group. Huperzine A was abbreviated as HupA. Scale bar: 50  $\mu$ m.

doi:10.1371/journal.pone.0128366.g002

rescued the decrease of ATP level (p < 0.05 vs oligomeric A $\beta_{42}$ -treated group). There was no significant difference between control group and huperzine A treated alone group (p > 0.05).

ROS trigger the oxidative stress in cells and reflect the functional status of mitochondria. We detected the accumulated ROS with the probe H<sub>2</sub>DCF-diacetate to find out whether huperzine A could decrease the ROS level. As compared with control group, oligomeric A $\beta_{42}$ -exposed neurons showed higher DCF fluorescence intensity (Fig 3B, p < 0.05). Huperzine A treatment significantly reduced DCF fluorescence intensity (p < 0.05 vs oligomeric A $\beta_{42}$ -



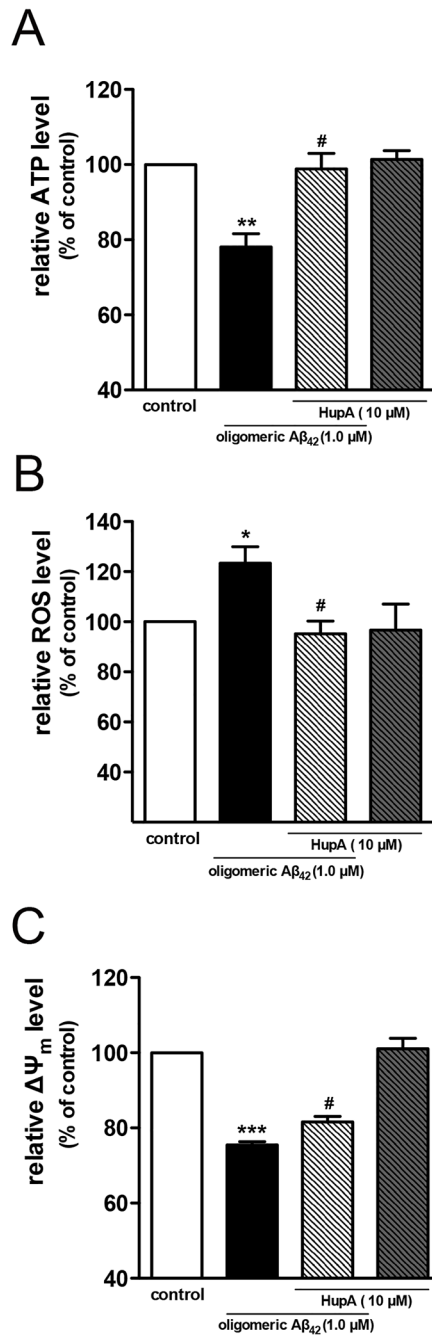


**Fig 3. Huperzine A ameliorated oligomeric A $\beta_{42}$  induced ATP reduction (A), ROS overproduction (B) and mitochondrial membrane potential decrease (C).** N = 3 for ATP assay, N = 4 for ROS assay, N = 4 for  $\Delta\Psi_m$  assay. Data were shown as mean  $\pm$  SEM. \* $p$  < 0.05, \*\* $p$  < 0.01, \*\*\* $p$  < 0.001 vs control group; # $p$  < 0.05 vs oligomeric A $\beta_{42}$ -treated group. Huperzine A was abbreviated as HupA.

doi:10.1371/journal.pone.0128366.g003

treated group). Similar to the effects observed in ATP assay, huperzine A treatment alone did not change the ROS level of neurons ( $p > 0.05$ ).

Mitochondrial membrane potential is a sensitive indicator of mitochondrial stress, and the maintenance of  $\Delta\Psi_m$  is very important to energy conversion and other signaling pathways. We

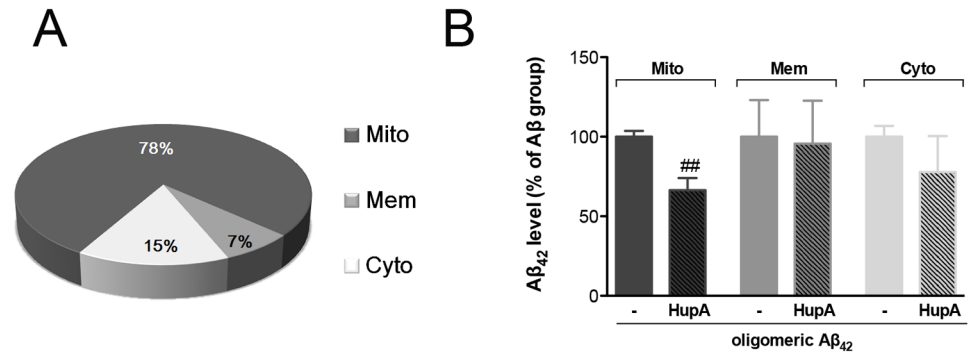


**Fig 4. Huperzine A decreased mitochondrial accumulation of A $\beta$ <sub>42</sub>.** A. The schematic diagram of the proportion of mitochondria-enriched fraction A $\beta$ <sub>42</sub> in total intracellular A $\beta$ <sub>42</sub>. B. Effect of huperzine A on the level of A $\beta$ <sub>42</sub> in different subcellular fractions (N = 4). Data were normalized by A $\beta$ <sub>42</sub>-treated group and shown as mean  $\pm$  SEM. ##p < 0.01 vs A $\beta$ <sub>42</sub> group. Huperzine A, mitochondria-enriched fraction, membrane fraction, cytosol fraction were respectively abbreviated as HupA, Mito, Mem, Cyto.

doi:10.1371/journal.pone.0128366.g004

assessed whether huperzine A was involved in the stability of  $\Delta\Psi_m$  using the JC-1 dye. As shown in Fig 3C, the  $\Delta\Psi_m$  of oligomeric A $\beta$ <sub>42</sub>-treated group dropped over 20% as compared with the control group (p < 0.001 vs vehicle treated control group). Huperzine A mildly but statistical significantly (about 10%) ameliorated the abnormal decrease of  $\Delta\Psi_m$  (Fig 3C, p < 0.05 vs oligomeric A $\beta$ <sub>42</sub>-treated group).

### Huperzine A decreased mitochondrial accumulation of A $\beta$ <sub>42</sub>

We separated mitochondria-enriched fraction, membrane fraction and cytosol fraction according to reported biochemical methods [32] and measured the A $\beta$  level of different fractions through ELISA assay. We found that the majority of intracellular A $\beta$  (about 78%) was distributed in the mitochondria-enriched fraction (Fig 4A). Huperzine A treatment significantly decreased the level of A $\beta$  distributed in mitochondria-enriched fraction (p < 0.001 vs oligomeric A $\beta$ <sub>42</sub>-treated group). Meanwhile, the A $\beta$  level of membrane and cytosol fractions was not significantly influenced by huperzine A treatment (Fig 4B).

To further confirm the results of mitochondrial A $\beta$ , we applied mitotracker probe to label mitochondria of primary neurons. As shown in Fig 5, HiLyte-A $\beta$ <sub>42</sub> (green fluorescence) colocalized well with mitotracker (red fluorescence), and huperzine A treatment decreased fluorescent signals of HiLyte-A $\beta$ <sub>42</sub> and mitochondria colocalization, which was similar as the result obtained by ELISA.

### Discussion

More and more attentions have been attracted on addressing the contribution of intracellular A $\beta$  in A $\beta$  oligomers-induced neurotoxicity [7, 39], yielding vigorously growing researches on discovering associated novel therapeutic strategies for AD based on “A $\beta$  cascade hypothesis”, during which employing small active molecules with potent pharmacological efficacy as probe is usually considered as an effective way [40]. As an extension of previous studies, we demonstrate for the first time that huperzine A, a natural product, possesses potent alleviative effect on oligomeric A $\beta$ <sub>42</sub>-induced neuronal damage, which is closely associated with the reduced level of intracellular A $\beta$  especially mitochondrial A $\beta$ , as well as the ameliorated mitochondrial function.

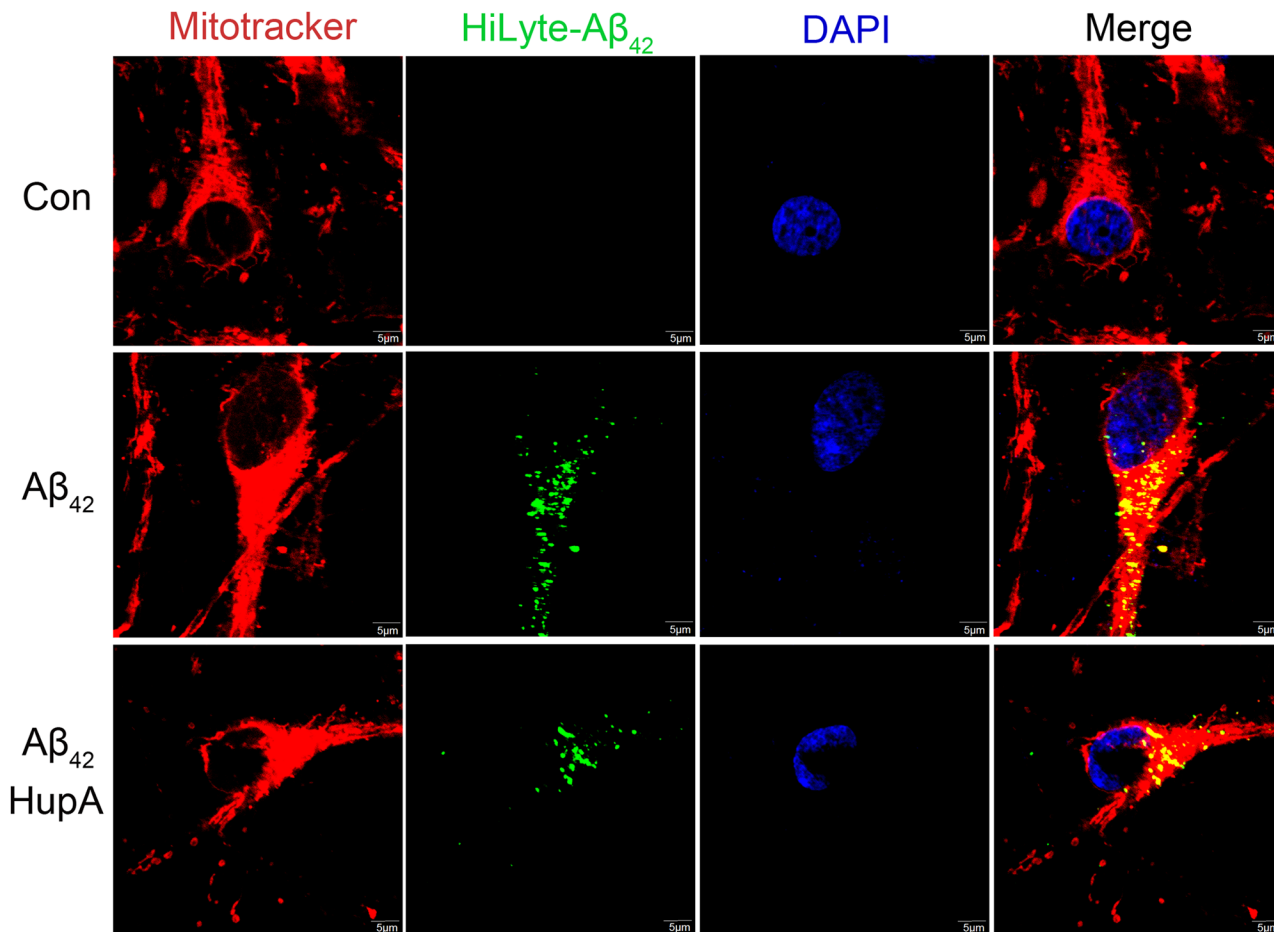


**Fig 5. Huperzine A decreased HiLyte-A $\beta_{42}$  fluorescent signals colocalized with mitochondrial marker in primary rat neurons.** The representative confocal microscopy figures of each group. Scale bar: 5  $\mu$ m.

doi:10.1371/journal.pone.0128366.g005

A number of investigators now propose that A $\beta$  oligomers, rather than A $\beta$  fibers, may be mainly responsible for neuronal synaptic dysfunction both *in vivo* and *in vitro*, which ultimately induce neuronal network disruption [41]. On the other hand, considerable studies have demonstrated that A $\beta_{42}$  is easier to form aggregates than A $\beta_{40}$  [42, 43] and is the predominant component of senile plaques [44]. We therefore evaluate the effects of huperzine A on primary neuronal damage induced by oligomeric A $\beta_{42}$ . Consistent with previous findings that 1  $\mu$ M A $\beta$  oligomers notably induced the damage of primary cultured neurons [45, 46], we also observed that oligomeric A $\beta_{42}$  significantly reduced MTT absorbance (Fig 1A). Post-administration of huperzine A significantly reversed the decreased MTT absorbance of primary cortical neurons induced by oligomeric A $\beta_{42}$  exposure (Fig 1A), which was similar with our previous results in various cell lines and primary cortical neurons treated with the active fragment A $\beta$  [15, 16]. No significant difference of SRB absorbance was found between each group (Fig 1B). The discrepancy between the results of MTT and SRB assays might be due to the different rationales behind the two methods: MTT assay measures the activity of succinate dehydrogenase—to reflect the metabolic activity of cells [47, 48], while SRB assay is based on the quantitative staining of cellular proteins—to reflect the cell number or density [49]. Therefore, the results of MTT and

SRB assays demonstrated that oligomeric A $\beta_{42}$  exposure significantly reduced the cell viability without causing obviously loss of primary neurons under our experimental conditions and the protective effect of huperzine A on the cell viability was not attributed to the cellular proliferation. Above results further suggested that the toxic effect of oligomeric A $\beta_{42}$  and the protective effect of huperzine A may be very likely associated with mitochondrial function, as succinate dehydrogenase, detected in MTT assay, is a key enzyme of TCA cycle. It is worth mentioning that it was the first time we administrated huperzine A after the insult of exogenous A $\beta$ , and the results will enrich our knowledge of the beneficial profiles of huperzine A in preventing or remedying A $\beta$ -associated neurodegeneration.

A growing body of evidence indicates that intracellular A $\beta$  is more toxic than extracellular A $\beta$  [50, 51] and the level of intraneuronal A $\beta$  is positively correlated with neuritic damage and synaptic alternations [52]. Therefore, intracellular A $\beta$  could be one of the novel therapeutic targets for the treatment of AD, however, only a few interventions have been identified to specifically reduce the accumulation of A $\beta$  intraneuronally and ameliorate the intracellular A $\beta$  neurotoxicity [53]. One of the obstacles for efficient discovery of active compounds is the paucity of studies showing a convincing link between intracellular A $\beta$  and neuronal death, we therefore systematically evaluated the changes of intraneuronal accumulation of A $\beta$  in primary cortical neurons applying synthetic and oligomeric A $\beta_{42}$ . In our work, oligomeric A $\beta$  accumulated into neurons time- and dose-dependently and correlated well with cell viability (Figure C in S1 File), which was consistent with earlier reports [32, 54]. Interestingly, by employing aforementioned cellular model, we demonstrated the co-occurrence of beneficial effects of huperzine A on neuronal survival and reduction of intracellular A $\beta$  level. Our data suggest that the potent effect of huperzine A on reducing intracellular A $\beta$  accumulation may effectively contribute to the protective effects of huperzine A against oligomeric A $\beta_{42}$ -induced neurotoxicity.

Mitochondria are believed as the major subcellular organelle for intracellular A $\beta$  accumulation [21, 32], although A $\beta$  also distributes in other sub-cellular compartments [55–57]. Similar as previous study [32], our results confirmed that mitochondria possessed the major part of intracellular A $\beta$  (Fig 4A). Moreover, it is also reported that exogenous A $\beta$  can be internalized into cells and colocalize with mitochondrial markers, which strongly influence mitochondrial respiratory function, ROS production rate, and mitochondria membrane potential [58, 59]. In our study, we firstly verified that the significant effects of huperzine A treatment on A $\beta_{42}$  induced mitochondrial dysfunction, as determined by ATP, ROS and mitochondria membrane potential measurement, happened concurrently with the decreased level of mitochondrial A $\beta_{42}$  (Figs 4 and 5). Above results suggest that the beneficial role of huperzine A against oligomeric A $\beta_{42}$ -induced neuronal injury may be closely associated with its protection on mitochondria, which may be attributed to the reduced level of mitochondrial A $\beta$ .

Considerable efforts have been put on impeding intracellular A $\beta$  neurotoxicity through reducing the accumulation of intracellular A $\beta$ . It is reported that the amount of intracellular A $\beta$  could be influenced by various factors involved in A $\beta$ -import process and A $\beta$ -degrading process [7, 21], while blocking the entrance of extracellular A $\beta$  into cytosol [53] and accelerating the clearance of intracellular A $\beta$  [60] are considered as the two major intervention strategies. Our preliminary study found that the A $\beta$  level in media of huperzine A-treated neurons showed increased tendency compared with that of A $\beta$ -treated alone neurons. In our experiment, A $\beta$  level in media was twenty-time higher than that in cell lysate, which should be sufficient for cellular uptake (data not shown). What's more, huperzine A hardly influenced A $\beta$ -degrading pathway in APP/PS1 transgenic mice according to our previous work [61]. Taken together, the reduction of intracellular A $\beta$  level after huperzine A treatment was unlikely attributed to the degradation of A $\beta$ . The precise mechanisms underlying the beneficial effects of huperzine A on reducing intracellular A $\beta$  accumulation and neurotoxicity remain to be

explored in future study. Nevertheless, our results provide important clues for an alternative way to hold back the progressing of intracellular A $\beta$  neurotoxicity through decreasing the accumulation of intracellular or mitochondrial A $\beta$ . What's more, our results shed more light on the pharmacological effects of huperzine A, which may be used as a pharmacological probe either for developing anti-AD drugs or clarifying potential therapeutic targets against A $\beta$  neurotoxicity.

## Supporting Information

**S1 File. Supporting figures.** Aggregation state of A $\beta_{42}$  (**Figure A**). Purity determination of subcellular fractions (**Figure B**). Intracellular A $\beta_{42}$  accumulation and correlation analysis with cell viability (**Figure C**). The nonspecific band detected by 6E10 antibody (**Figure D**). (DOCX)

## Acknowledgments

This work was supported by the National Natural Science Foundation of China (No 81173034), the National Science & Technology Major Project “Key New Drug Creation and Manufacturing Program” of China (No. 2012ZX09301001-004), and the Ministry of Science and Technology of China (No 2011CB510004).

## Author Contributions

Conceived and designed the experiments: HYZ. Performed the experiments: YL LY CYY MYQ. Analyzed the data: YL LY. Contributed reagents/materials/analysis tools: HYY HLJ XCT HYZ. Wrote the paper: YL HYZ.

## References

1. Sosa-Ortiz AL, Acosta-Castillo I, Prince MJ. Epidemiology of dementias and Alzheimer's disease. *Arch Med Res*. 2012; 43(8):600–608. PMID: [23159715](#). doi: [10.1016/j.arcmed.2012.11.003](#)
2. Karran E, Mercken M, De Strooper B. The amyloid cascade hypothesis for Alzheimer's disease: an appraisal for the development of therapeutics. *Nat Rev Drug Discov*. 2011; 10(9):698–712. PMID: [21852788](#). doi: [10.1038/nrd3505](#)
3. Palop JJ, Mucke L. Amyloid-beta-induced neuronal dysfunction in Alzheimer's disease: from synapses toward neural networks. *Nat Neurosci*. 2010; 13(7):812–818. PMID: [20581818](#). doi: [10.1038/nn.2583](#)
4. Hardy J, Selkoe DJ. The amyloid hypothesis of Alzheimer's disease: progress and problems on the road to therapeutics. *Science*. 2002; 297(5580):353–356. PMID: [12130773](#).
5. Billings LM, Oddo S, Green KN, McGaugh JL, LaFerla FM. Intraneuronal Abeta causes the onset of early Alzheimer's disease-related cognitive deficits in transgenic mice. *Neuron*. 2005; 45(5):675–688. PMID: [15748844](#).
6. Gouras GK, Almeida CG, Takahashi RH. Intraneuronal Abeta accumulation and origin of plaques in Alzheimer's disease. *Neurobiol Aging*. 2005; 26(9):1235–1244. PMID: [16023263](#).
7. LaFerla FM, Green KN, Oddo S. Intracellular amyloid-beta in Alzheimer's disease. *Nat Rev Neurosci*. 2007; 8(7):499–509. PMID: [17551515](#).
8. Takahashi RH, Capetillo-Zarate E, Lin MT, Milner TA, Gouras GK. Co-occurrence of Alzheimer's disease ss-amyloid and tau pathologies at synapses. *Neurobiol Aging*. 2010; 31(7):1145–1152. PMID: [18771816](#). doi: [10.1016/j.neurobiolaging.2008.07.021](#)
9. Gouras GK, Tampellini D, Takahashi RH, Capetillo-Zarate E. Intraneuronal beta-amyloid accumulation and synapse pathology in Alzheimer's disease. *Acta Neuropathol*. 2010; 119(5):523–541. PMID: [20354705](#). doi: [10.1007/s00401-010-0679-9](#)
10. Umeda T, Tomiyama T, Sakama N, Tanaka S, Lambert MP, Klein WL, et al. Intraneuronal amyloid beta oligomers cause cell death via endoplasmic reticulum stress, endosomal/lysosomal leakage, and mitochondrial dysfunction in vivo. *J Neurosci Res*. 2011; 89(7):1031–1042. PMID: [21488093](#). doi: [10.1002/jnr.22640](#)

11. Wang R, Yan H, Tang XC. Progress in studies of huperzine A, a natural cholinesterase inhibitor from Chinese herbal medicine. *Acta Pharmacol Sin.* 2006; 27(1):1–26. PMID: [16364207](#).
12. Zhang HY, Tang XC. Neuroprotective effects of huperzine A: new therapeutic targets for neurodegenerative disease. *Trends Pharmacol Sci.* 2006; 27(12):619–625. PMID: [17056129](#).
13. Zhang HY, Yan H, Tang XC. Non-cholinergic effects of huperzine A: beyond inhibition of acetylcholinesterase. *Cell Mol Neurobiol.* 2008; 28(2):173–183. PMID: [17657601](#).
14. Gao X, Tang XC. Huperzine A attenuates mitochondrial dysfunction in beta-amyloid-treated PC12 cells by reducing oxygen free radicals accumulation and improving mitochondrial energy metabolism. *J Neurosci Res.* 2006; 83(6):1048–1057. PMID: [16493671](#).
15. Zhang HY, Liang YQ, Tang XC, He XC, Bai DL. Stereoselectivities of enantiomers of huperzine A in protection against beta-amyloid(25–35)-induced injury in PC12 and NG108-15 cells and cholinesterase inhibition in mice. *Neurosci Lett.* 2002; 317(3):143–146. PMID: [11755260](#).
16. Xiao XQ, Zhang HY, Tang XC. Huperzine A attenuates amyloid beta-peptide fragment 25-35-induced apoptosis in rat cortical neurons via inhibiting reactive oxygen species formation and caspase-3 activation. *J Neurosci Res.* 2002; 67(1):30–36. PMID: [11754078](#).
17. Walsh DM, Selkoe DJ. A beta oligomers—a decade of discovery. *J Neurochem.* 2007; 101(5):1172–1184. PMID: [17286590](#).
18. Klein WL, Krafft GA, Finch CE. Targeting small A $\beta$  oligomers: the solution to an Alzheimer's disease conundrum? *Trends Neurosci.* 2001; 24(4):219–224. PMID: [11250006](#).
19. Ferreira ST, Vieira MN, De Felice FG. Soluble protein oligomers as emerging toxins in Alzheimer's and other amyloid diseases. *IUBMB Life.* 2007; 59(4–5):332–345. PMID: [17505973](#).
20. Caspersen C, Wang N, Yao J, Sosunov A, Chen X, Lustbader JW, et al. Mitochondrial A $\beta$ : a potential focal point for neuronal metabolic dysfunction in Alzheimer's disease. *FASEB J.* 2005; 19(14):2040–2041. PMID: [16210396](#).
21. Pinho CM, Teixeira PF, Glaser E. Mitochondrial import and degradation of amyloid-beta peptide. *Biochim Biophys Acta.* 2014; 1837(7):1069–1074. PMID: [24561226](#). doi: [10.1016/j.bbabi.2014.02.007](#)
22. Manczak M, Anekonda TS, Henson E, Park BS, Quinn J, Reddy PH. Mitochondria are a direct site of A $\beta$  accumulation in Alzheimer's disease neurons: implications for free radical generation and oxidative damage in disease progression. *Hum Mol Genet.* 2006; 15(9):1437–1449. PMID: [16551656](#).
23. Cha MY, Han SH, Son SM, Hong HS, Choi YJ, Byun J, et al. Mitochondria-specific accumulation of amyloid beta induces mitochondrial dysfunction leading to apoptotic cell death. *PLoS One.* 2012; 7(4):e34929. PMID: [22514691](#). doi: [10.1371/journal.pone.0034929](#)
24. Rosales-Corral S, Acuna-Castroviejo D, Tan DX, Lopez-Atarés G, Cruz-Ramos J, Muñoz R, et al. Accumulation of exogenous amyloid-beta peptide in hippocampal mitochondria causes their dysfunction: a protective role for melatonin. *Oxid Med Cell Longev.* 2012; 2012:843649. PMID: [22666521](#). doi: [10.1155/2012/843649](#)
25. He Y, Cui J, Lee JC, Ding S, Chalimoniuk M, Simonyi A, et al. Prolonged exposure of cortical neurons to oligomeric amyloid-beta impairs NMDA receptor function via NADPH oxidase-mediated ROS production: protective effect of green tea (-)-epigallocatechin-3-gallate. *ASN Neuro.* 2011; 3(1):e00050. PMID: [21434871](#). doi: [10.1042/AN20100025](#)
26. Ryan DA, Narrow WC, Federoff HJ, Bowers WJ. An improved method for generating consistent soluble amyloid-beta oligomer preparations for in vitro neurotoxicity studies. *J Neurosci Methods.* 2010; 190(2):171–179. PMID: [20452375](#). doi: [10.1016/j.jneumeth.2010.05.001](#)
27. Du J, Feng L, Yang F, Lu B. Activity- and Ca(2+)-dependent modulation of surface expression of brain-derived neurotrophic factor receptors in hippocampal neurons. *J Cell Biol.* 2000; 150(6):1423–1434. PMID: [10995446](#).
28. Ray B, Bailey JA, Sarkar S, Lahiri DK. Molecular and immunocytochemical characterization of primary neuronal cultures from adult rat brain: Differential expression of neuronal and glial protein markers. *J Neurosci Methods.* 2009; 184(2):294–302. PMID: [19720084](#). doi: [10.1016/j.jneumeth.2009.08.018](#)
29. Agostinho P, Oliveira CR. Involvement of calcineurin in the neurotoxic effects induced by amyloid-beta and prion peptides. *Eur J Neurosci.* 2003; 17(6):1189–1196. PMID: [12670307](#).
30. Choi H, Park HH, Koh SH, Choi NY, Yu HJ, Park J, et al. Coenzyme Q10 protects against amyloid beta-induced neuronal cell death by inhibiting oxidative stress and activating the P13K pathway. *Neurotoxicology.* 2012; 33(1):85–90. PMID: [22186599](#). doi: [10.1016/j.neuro.2011.12.005](#)
31. Sarafian TA, Montes C, Imura T, Qi J, Coppola G, Geschwind DH, et al. Disruption of astrocyte STAT3 signaling decreases mitochondrial function and increases oxidative stress in vitro. *PLoS One.* 2010; 5(3):e9532. PMID: [20224768](#). doi: [10.1371/journal.pone.0009532](#)

32. Takuma K, Fang F, Zhang W, Yan S, Fukuzaki E, Du H, et al. RAGE-mediated signaling contributes to intraneuronal transport of amyloid-beta and neuronal dysfunction. *Proc Natl Acad Sci U S A*. 2009; 106(47):20021–20026. PMID: [19901339](#). doi: [10.1073/pnas.0905686106](#)
33. Reed MN, Hofmeister JJ, Jungbauer L, Welzel AT, Yu C, Sherman MA, et al. Cognitive effects of cell-derived and synthetically derived Abeta oligomers. *Neurobiol Aging*. 2011; 32(10):1784–1794. PMID: [20031278](#). doi: [10.1016/j.neurobiolaging.2009.11.007](#)
34. Hung LW, Ciccotosto GD, Giannakis E, Tew DJ, Perez K, Masters CL, et al. Amyloid-beta peptide (Abeta) neurotoxicity is modulated by the rate of peptide aggregation: Abeta dimers and trimers correlate with neurotoxicity. *J Neurosci*. 2008; 28(46):11950–11958. PMID: [19005060](#). doi: [10.1523/JNEUROSCI.3916-08.2008](#)
35. Benilova I, Karran E, De Strooper B. The toxic Abeta oligomer and Alzheimer's disease: an emperor in need of clothes. *Nat Neurosci*. 2012; 15(3):349–357. PMID: [22286176](#). doi: [10.1038/nn.3028](#)
36. Bhaskar K, Miller M, Chludzinski A, Herrup K, Zagorski M, Lamb BT. The PI3K-Akt-mTOR pathway regulates Abeta oligomer induced neuronal cell cycle events. *Mol Neurodegener*. 2009; 4:14. PMID: [19291319](#). doi: [10.1186/1750-1326-4-14](#)
37. Halle A, Hornung V, Petzold GC, Stewart CR, Monks BG, Reinheckel T, et al. The NALP3 inflammasome is involved in the innate immune response to amyloid-beta. *Nat Immunol*. 2008; 9(8):857–865. PMID: [18604209](#). doi: [10.1038/ni.1636](#)
38. Kanekiyo T, Zhang J, Liu Q, Liu CC, Zhang L, Bu G. Heparan sulphate proteoglycan and the low-density lipoprotein receptor-related protein 1 constitute major pathways for neuronal amyloid-beta uptake. *J Neurosci*. 2011; 31(5):1644–1651. PMID: [21289173](#). doi: [10.1523/JNEUROSCI.5491-10.2011](#)
39. Wirths O, Bayer TA. Intraneuronal Abeta accumulation and neurodegeneration: lessons from transgenic models. *Life Sci*. 2012; 91(23–24):1148–1152. PMID: [22401905](#). doi: [10.1016/j.lfs.2012.09.022](#)
40. Belluti F, Rampa A, Gobbi S, Bisi A. Small-molecule inhibitors/modulators of amyloid-beta peptide aggregation and toxicity for the treatment of Alzheimer's disease: a patent review (2010–2012). *Expert Opin Ther Pat*. 2013; 23(5):581–596. PMID: [23425062](#). doi: [10.1517/13543776.2013.772983](#)
41. Kaye R, Lasagna-Reeves CA. Molecular mechanisms of amyloid oligomers toxicity. *J Alzheimers Dis*. 2013; 33 Suppl 1:S67–78. PMID: [22531422](#). doi: [10.3233/JAD-2012-129001](#)
42. Bitan G, Kirkitadze MD, Lomakin A, Vollers SS, Benedek GB, Teplow DB. Amyloid beta-protein (Abeta) assembly: Abeta 40 and Abeta 42 oligomerize through distinct pathways. *Proc Natl Acad Sci U S A*. 2003; 100(1):330–335. PMID: [12506200](#).
43. Selkoe DJ. Alzheimer's disease: genes, proteins, and therapy. *Physiol Rev*. 2001; 81(2):741–766. PMID: [11274343](#).
44. Stine WB Jr., Dahlgren KN, Krafft GA, LaDu MJ. In vitro characterization of conditions for amyloid-beta peptide oligomerization and fibrillogenesis. *J Biol Chem*. 2003; 278(13):11612–11622. PMID: [12499373](#).
45. Liang JH, Du J, Xu LD, Jiang T, Hao S, Bi J, et al. Catalpol protects primary cultured cortical neurons induced by Abeta(1–42) through a mitochondrial-dependent caspase pathway. *Neurochem Int*. 2009; 55(8):741–746. PMID: [19631247](#). doi: [10.1016/j.neuint.2009.07.004](#)
46. Resende R, Ferreira E, Pereira C, Resende de Oliveira C. Neurotoxic effect of oligomeric and fibrillar species of amyloid-beta peptide 1–42: involvement of endoplasmic reticulum calcium release in oligomer-induced cell death. *Neuroscience*. 2008; 155(3):725–737. PMID: [18621106](#). doi: [10.1016/j.neuroscience.2008.06.036](#)
47. Lobner D. Comparison of the LDH and MTT assays for quantifying cell death: validity for neuronal apoptosis? *J Neurosci Methods*. 2000; 96(2):147–152. PMID: [10720679](#).
48. Burton JD. The MTT assay to evaluate chemosensitivity. *Methods Mol Med*. 2005; 110:69–78. PMID: [15901928](#).
49. Voigt W. Sulforhodamine B assay and chemosensitivity. *Methods Mol Med*. 2005; 110:39–48. PMID: [15901925](#).
50. Kienlen-Campard P, Miolet S, Tasiaux B, Octave JN. Intracellular amyloid-beta 1–42, but not extracellular soluble amyloid-beta peptides, induces neuronal apoptosis. *J Biol Chem*. 2002; 277(18):15666–15670. PMID: [11861655](#).
51. Zhang Y, McLaughlin R, Goodyer C, LeBlanc A. Selective cytotoxicity of intracellular amyloid beta peptide 1–42 through p53 and Bax in cultured primary human neurons. *J Cell Biol*. 2002; 156(3):519–529. PMID: [11815632](#).
52. Takahashi RH, Capetillo-Zarate E, Lin MT, Milner TA, Gouras GK. Accumulation of intraneuronal beta-amyloid 42 peptides is associated with early changes in microtubule-associated protein 2 in neurites and synapses. *PLoS One*. 2013; 8(1):e51965. PMID: [23372648](#). doi: [10.1371/journal.pone.0051965](#)

53. Maezawa I, Hong HS, Wu HC, Battina SK, Rana S, Iwamoto T, et al. A novel tricyclic pyrone compound ameliorates cell death associated with intracellular amyloid-beta oligomeric complexes. *J Neurochem*. 2006; 98(1):57–67. PMID: [16805796](#).
54. Song MS, Baker GB, Todd KG, Kar S. Inhibition of beta-amyloid1-42 internalization attenuates neuronal death by stabilizing the endosomal-lysosomal system in rat cortical cultured neurons. *Neuroscience*. 2011; 178:181–188. PMID: [21262324](#). doi: [10.1016/j.neuroscience.2010.12.055](#)
55. Choy RW, Cheng Z, Schekman R. Amyloid precursor protein (APP) traffics from the cell surface via endosomes for amyloid beta (A $\beta$ ) production in the trans-Golgi network. *Proc Natl Acad Sci U S A*. 2012; 109(30):E2077–2082. PMID: [22711829](#). doi: [10.1073/pnas.1208635109](#)
56. Yamazaki T, Chang TY, Haass C, Ihara Y. Accumulation and aggregation of amyloid beta-protein in late endosomes of Niemann-pick type C cells. *J Biol Chem*. 2001; 276(6):4454–4460. PMID: [11085995](#).
57. Liu RQ, Zhou QH, Ji SR, Zhou Q, Feng D, Wu Y, et al. Membrane localization of beta-amyloid 1–42 in lysosomes: a possible mechanism for lysosome labilization. *J Biol Chem*. 2010; 285(26):19986–19996. PMID: [20430896](#). doi: [10.1074/jbc.M109.036798](#)
58. Hansson Petersen CA, Alikhani N, Behbahani H, Wiehager B, Pavlov PF, Alafuzoff I, et al. The amyloid beta-peptide is imported into mitochondria via the TOM import machinery and localized to mitochondrial cristae. *Proc Natl Acad Sci U S A*. 2008; 105(35):13145–13150. PMID: [18757748](#). doi: [10.1073/pnas.0806192105](#)
59. Picone P, Nuzzo D, Caruana L, Scafidi V, Di Carlo M. Mitochondrial dysfunction: different routes to Alzheimer's disease therapy. *Oxid Med Cell Longev*. 2014; 2014:780179. PMID: [25221640](#). doi: [10.1155/2014/780179](#)
60. Guo J, Chang L, Zhang X, Pei S, Yu M, Gao J. Ginsenoside compound K promotes beta-amyloid peptide clearance in primary astrocytes via autophagy enhancement. *Exp Ther Med*. 2014; 8(4):1271–1274. PMID: [25187838](#).
61. Wang Y, Tang XC, Zhang HY. Huperzine A alleviates synaptic deficits and modulates amyloidogenic and nonamyloidogenic pathways in APP<sup>swe</sup>/PS1<sup>dE9</sup> transgenic mice. *J Neurosci Res*. 2012; 90(2):508–517. PMID: [22002568](#). doi: [10.1002/jnr.22775](#)